International Journal of Biological Macromolecules 140 (2019) 833–841

Contents lists available at ScienceDirect

International Journal of Biological Macromolecules

journal homepage: http://www.elsevier.com/locate/ijbiomac

Optimization of aqueous two-phase partitioning of *Aureobasidium pullulans* α-amylase via response surface methodology and investigation of its thermodynamic and kinetic properties

A.N. Ademakinwa [a,c,*], M.O. Agunbiade [b], Z.A. Ayinla [c,d], F.K. Agboola [c]

[a] Department of Physical and Chemical Sciences, Elizade University, Ilara-Mokin, Nigeria
[b] Biocatalysis and Technical Biology Research Group, Institute of Biomedical and Microbial Biotechnology, Cape Peninsula University of Technology, South Africa
[c] Department of Biochemistry and Molecular Biology, Obafemi Awolowo University, Ile-Ife, Nigeria
[d] Center for Biotechnology and Interdisciplinary Studies, Rensselaer Polytechnic, Troy, NY 12180, USA

ARTICLE INFO

Article history:
Received 22 July 2019
Received in revised form 16 August 2019
Accepted 18 August 2019
Available online 21 August 2019

Keywords:
α-Amylase
Aureobasidium pullulans
Thermodynamics
Kinetic
ATPS

ABSTRACT

Industrial enzymes such as α-amylase must be thermostable and also easily purified/concentrated. Hence, aqueous two-phase partitioning systems (ATPS) was exploited for the partitioning of α-amylase from *Aureobasidium pullulans* due to its numerous advantages over conventional purification strategy. *A. pullulans* α-amylase was partially purified using ATPS via response surface methodology (RSM). The potentials of the ATPS-purified enzyme for possible industrial application such as resistance to thermal inactivation was investigated in comparison with the crude enzyme. PEG-6000 was the polymer of choice for ATPS as it resulted in higher purification factor (PF), %yield (Y), and partition coefficient (PC). At optimum levels (% *w*/*v*) of 20, 12 and 7.5 for PEG-6000, sodium citrate and sodium chloride respectively, maximum PF, Y and PC of 4.2, 88%, and 9.9 respectively were obtained. The response model validation and reliability were established based on the closeness between the experimented and predicted values. The kinetic and thermodynamic parameters such as Q_{10}, $t_{1/2}$, k_d, D — value, E_d, ΔH_d^*, ΔG_d^* *and* ΔS_d^* of the ATPS-purified α-amylase indicated that it was thermostable at 50 to 60 °C compared to the crude α-amylase. A thermodynamically stable and ATPS-purified α-amylase from *A. pullulans* has properties easily applicable for most industrial processes.

1. Introduction

Amylases are one of the most important industrial hydrolytic enzymes because they are applicable in a wide array of industries such as starch liquefaction, paper pulping, food (cakes, fruit juices, brewing), detergents etc. [1]. The α-amylases hydrolyses the internal β-1, 4-glucosidic bonds in starch or other polysaccharides to give low molecular weight products. This enzyme is sourced from a host of bacteria, fungi and plants [2]. The α-amylase for industrial applications are mostly obtained from microorganisms and they must display some resistance to thermal denaturation. This had led to the increased demand for thermal stable α-amylase. Other important properties α-amylase for industrial applications must have include stability to pH, detergents, inhibitors etc. This will allow the enzymes to adapt to extreme conditions often found in most industries [3]. Another important feature desired in deploying α-amylase for most industrial application is the ease of purification from the fermented medium. The purification strategy used is often a significant factor as a complex/traditional purification approach might increase the cost of production. Most traditional processes of purification are laborious, entail many purification steps, loss of enzyme activity as well as reduced yield [4]. Hence a single step that encompasses a fast purification, economical and easily amenable is strongly desired. Aqueous two-phase systems offer a great alternative to the traditional purification process because it is easily adaptable and the potential for scale-up is great. Also, it combines both clarification of the crude enzyme homogenate, concentration of the enzyme as well as partial purification in a single process [5,6]. ATPS is mostly derived by mixing different polymers or a polymer and a salt in water at a higher known concentration. The many advantages offered by ATPS allows its use in industrial enzyme purification a necessity. The major advantage of ATPS is that it maintains the integrity (biological and protein functions) of the enzyme by minimizing the possible protein degradation. This characteristic feature of ATPS is possible because of the very high water content and the corresponding low interfacial tension [4,7]. This property of ATPS somehow confers thermodynamic stability to the enzyme as both phases are mild and not destructive to the enzyme [8]. ATPS has been employed for the purification of enzymes and other biomolecules. Often times the process of ATPS can be optimized as no

* Corresponding author at: Department of Physical and Chemical Sciences, Elizade University, Ilara-Mokin, Nigeria
E-mail address: adedeji.ademakinwa@elizadeuniversity.edu.ng (A.N. Ademakinwa).

https://doi.org/10.1016/j.ijbiomac.2019.08.159
0141-8130/

model provides a priori estimation of protein separation [9]. Optimal conditions are also determined after conducting the experiment. Using ATPS for protein purification, several critical parameters such as concentration of the polymers/salts, pH and temperature must be considered as they influence the recovery, yield, and purification factor. It is important to select correct composition of the ATPS during purification of target protein to obtain maximum yield and purification fold. Hence, the use of response surface methodology (RSM) as a tool for optimization. The RSM is a statistical approach that allows the optimal conditions from numerous independent variables to be obtained without conducting redundant and unnecessary experiments. Several authors have employed the technique of RSM for optimization of ATPS for α-amylase purification [4,7]. The use of ATPS for purification of α-amylase and other biomolecules under optimized conditions have been reported by several authors [4,7,10].

Enzymes for industrial applications such as α-amylase must be sourced from microorganisms (such as fungi, bacteria and yeasts) as they are cheaper to produce on a large-scale compared to plants. Numerous reports exists of α-amylase production from these organisms but very few exists for the fungus, *Aureobasidium pullulans*. *A. pullulans* produces a host of important industrial enzymes and it has the generally regarded as safe (GRAS) status. Hence the α-amylase obtained from *A. pullulans* could be useful in several food, beverage and other allied industries. In this study, α-amylase obtained from *A. pullulans* was partially purified using ATPS. As observed in our findings, very few reports exist on *A. pullulan* α-amylase. Mulay and Deopurkar [11] only focused on the purification *A. pullulan* α-amylase using conventional means as well as its bio-conjugation on gold nanoparticles. It is known that conventional protocols for purification of industrial enzymes results in lower yield, its cumbersome and often times the enzyme is diluted hence the need to focus on a simple strategy that combines simplicity, concentration and a high yield in a single step. The ATPS process employed in this study was optimized using response surface methodology (RSM) and factors such as the concentration of the polymers/salts which influence the purification fold, yield and recovery of the protein were investigated. Also, the potentials of the ATPS-purified enzyme to resist thermal denaturation in comparison with the crude α-amylase was investigated as a function of its kinetic and thermodynamic parameters. This is the first report of its kind that directly investigates the thermodynamic and kinetic parameters of α-amylase from *A. pullulans* that was partially purified using a non-conventional purification strategy. The thermodynamically stable ATPS-purified α-amylase would be better utilized in several industries where α-amylase- mediated starch hydrolysis is often employed.

2. Materials and methods

2.1. Materials

Polyethylene glycol (4000, 6000 and 8000), corn starch, maltose, sodium potassium tartrate, dinitrosalicyclic acid, glucose, Coomassie Brilliant Blue G-250 were purchased from Sigma-Aldrich, USA. The fungus, *A. pullulans,* used in this study was previously isolated from soil containing decayed plant litters and its molecular identification was by the sequencing of its internally transcribed spacer genomic regions (ITS 1 and 4). The nucleotide sequence was deposited in the GenBank database (accession number of KX023301) [12].

2.2. Methods

2.2.1. Microorganisms and culture conditions

A. pullulans was maintained on malt extract agar (MEA) and subcultured every 72 h at 25 °C. Agar plugs (10 mm) were obtained from the actively grown regions on the agar plate and they served as the inoculum.

2.2.2. α-Amylase production and extraction

Submerged fermentation was employed for the production of α-amylase in a medium containing (in g/100 ml): KH_2PO_4 (0.2) NaCl (0.2), starch (2), $CaCl_2$ (0.01), peptone (1) and $MgSO_4$ (0.1). The medium was maintained at pH 5.5. The medium was autoclaved at 121 psi for 5 min, cooled to room temperature (25C) and inoculated with 1 agar plug (10 mm). Further incubation was carried out for 7 days at 25 °C. The supernatant of the culture medium obtained by centrifuging at 4000 x g for 15 min served as the crude enzyme.

2.2.3. α-Amylase assay and determination of protein concentration

α-Amylase assay was carried out by incubating 1% starch and the diluted crude enzyme using methods described by Shukla and Singh [3]. The maltose released was quantified using the methods described by Miller et al. [13]. One unit of α-amylase was described as the amount of the enzyme that releases one microgram of maltose from starch per minute under the standard assay conditions.

Protein concentration was determined using the methods described by Bradford [14] with bovine serum albumin as standard.

2.2.4. Aqueous two-phase partitioning systems

2.2.4.1. Screening of PEG molecular weight on α-amylase partitioning. Different molecular weights of PEG (4000, 6000 and 8000) were screened for α-amylase partitioning. The composition (in final concentration) of the polymer and salts were 24, 7.5 and 2% respectively for the PEG, sodium citrate and sodium chloride respectively. For the ATPS process, the polymer/salts were added to 10 ml of the crude α-amylase supernatant and dissolved via gentle mixing using a spatula. Phase separation occurred after 1 h and the volumes of the upper and lower phases were noted. The top phase was separated from the bottom phase using a sterile Pasteur pipette and the volumes of both phases noted. α-Amylase activity and protein concentration were determined for both phases [4,7]. All experiments were carried out at room temperature (25 °C). The purification fold, α-amylase partition coefficient and yield (%) were determined from the upper phase. The formulae are shown below

$$\text{Specific Activity } (\rho) = \frac{\text{Activity}}{\text{Protein Concentration}}$$

$$\text{Partition Coefficient } (\mu) = {}^{\text{Activity in the Upper Phase}} \Big/ _{\text{Activity in the Lower Phase}}$$

$$\text{Purification Fold } (\omega) = \frac{\text{Specific Activiy in Upper Phase}}{\text{Specific Activity in Lower Phase}}$$

$$\%\text{Yield} = \frac{100}{1 + ({}^{1}/_{(\beta \cdot \mu)})}$$

$$\text{Volume Ratio } (\beta) = \frac{\text{Volume of Upper Phase}}{\text{Volume of Lowe Phase}}$$

2.2.4.2. Optimization of aqueous two-phase partitioning systems via response surface methodology. The RSM involves a well-defined experimental design, statistical modeling to evaluate the interactions and optimization of the process parameters (independent variables) to obtain an optimum response. In this study, Box-Behnken was used for the optimization of the extraction of α-amylase using aqueous two phase partitioning. The independent variables were expressed as coded value. The real and coded values are indicated in Table 1. The final concentrations of PEG, sodium citrate and sodium chloride were chosen as the very significant independent variables affecting the purification of α-amylase when aqueous two phase systems are used. In this study, the dependent variables (responses) were purification fold, α-amylase partition coefficient and yield (%) and they were determined

Table 1
Variable ranges used for the Box-Behnken response surface methodology experimental design.

Symbol	Name of variable	Range
A	NaCl (w/v)	5–10
B	Sodium citrate (w/v)	5–15
B	PEG-6000 (w/v)	10–25

for the upper phase after each experimental runs. There were sixteen individual experimental runs and the independent variables were varied at 3 different levels (Table 2). The modeling and analysis were analyzed using Design-Expert (version 6.0, Stat-Ease Inc. Minneapolis, USA). A second-order polynomial equation and data-fitting by multiple regression techniques. The model equation for analysis and calculation of the predicted response is given in equation below:

$$X = \propto_o + \sum_{j=1}^{k} \propto_j y_j + \sum_{j=1}^{k} \propto_{jj} y_j^2 + \sum_{i<} \sum_{j=2}^{k} \propto_{ij} y_i y_j \quad (1)$$

where, X represents the response variable, $\propto_o$ is the intercept coefficient linear, $\propto_i$is the coefficient linear effect, $\propto_{jj}$ is the coefficient of quadratic effect and $\propto_{ij}$ are the regression coefficients for the interaction effects, and $y_i y_j$ are the coded independent variables.

2.2.4.3. Model and regression analysis. Analysis of variance was used for the determination of significant variables influencing the partitioning of α-amylase in the PEG-rich upper phase. The data obtained from the experimental design was fitted to second order models using multiple regression techniques. The predicted response was derived from the polynomial model and it's a result of the interaction between the independent variables. The polynomial model was represented by the 3D response surface plots to determine the very significant variables influencing the three responses studied. The 3D response surface plots were drawn in such a manner that one of the independent variables was held constant at the center point while the remaining two variables vary within the experimental range. The numerical and graphical optimization was used to determine the optimum levels of the independent variables that provides the desired responses.

2.2.5. Sodium dodecylsulphate polyacrylamide gel electrophoresis (SDS-PAGE) of the crude and ATPS-partially purified α-amylase

SDS-PAGE of both crude and ATPS-purified α-amylase was carried out according to the method described by Laemmli [15]. The gel slabs were prepared with the upper stacking gel (4%) and lower resolving gel (12%). After the electrophoresis, the resolved bands on the gel were visualized using Coomassie brilliant blue R-250.

2.2.6. Effect of pH and temperature

The reaction (α-amylase) mixture was incubated at various temperatures (30 to 90 °C) and the enzymatic activity routinely determined using the methods described in Section 2.2.3.

The effects of pH was studied from the range of 4–10 using the following buffers: 5 mM acetate buffer (4–5); 5 mM phosphate buffer (6–8) and Tris-HCl buffer (9–10) [3]. The reaction mixture at the specific pH was incubated at the optimum temperature (50 °C) for the α-amylase assay.

2.2.7. Thermal stability studies and determination of kinetic and thermodynamic parameters

For the thermal stability studies, the dialyzed ATPS fraction was subjected to incubation at different temperatures ranging from 40 to 80 °C for 5 h. Aliquots were withdrawn every hour and used in α-amylase assay.

The thermal inactivation of enzymes is often explained using first-order reaction kinetics [16,17] as described by Eq. (2)

$$v_{d=} k_d E$$

v_d: rate of enzyme inactivation,
k_d: first-order constant and
E: enzyme concentration
The k_d is defined in Eq. (2)

$$k_d = Ae^{-E_d/RT} \quad (2)$$

A: pre-exponential factor,
E_d: activation energy of denaturation,
R: universal gas constant and
T: absolute temperature

The k_d was estimated from the slopes of the plot of In (ϖ) against temperature (T).

Table 2
Design and the response (purification factor, yield and partition coefficient) values.

Runs	Factors (real and coded)			Response(s)		
	NaCl (w/v)	Sodium citrate (w/v)	PEG-6000 (w/v)	Purification factor	Yield (%)	Partition coefficient
1	1.00 (10)	0.00 (10)	−1.00 (10)	0.6	18.4	7.7
2	0.00 (7.5)	0.00 (10)	0.00 (20)	4.0	86.9	9.3
3	0.00 (7.5)	0.00 (10)	0.00 (20)	4.1	87.9	9.2
4	0.00 (7.5)	0.00 (10)	0.00 (20)	4.2	88.9	9.5
5	0.00 (7.5)	0.00 (10)	0.00 (20)	4.1	87.9	9.5
6	−1.00 (5.0)	1.00 (15)	0.00 (20)	2.9	63.4	7.5
7	0.00 (7.5)	1.00 (15)	−1.00 (10)	2.0	43.0	7.5
8	0.00 (7.5)	−1.00 (5)	−1.00 (10)	1.2	20.5	7.6
9	−1.00 (5.0)	0.00 (10)	1.00 (25)	2.8	60.3	6.9
10	0.00 (7.5)	0.00 (10)	0.00 (20)	4.0	86.9	9.2
11	−1.00 (5.0)	0.00 (10)	−1.00 (10)	1.8	38.8	8.3
12	0.00 (7.5)	−1.00 (5)	1.00 (25)	2.2	46.0	7.4
13	1.00 (10)	−1.00 (5)	0.00 (20)	0.95	20.4	8.1
14	1.00 (10)	1.00 (10)	0.00 (20)	1.6	15.3	8.1
15	0.00 (7.5)	1.00 (10)	1.00 (25)	2.7	58.2	7.3
16	−1.00 (5)	−1.00 (5)	0.00 (20)	1.1	24.5	7.5
17	1.00 (10)	0.00 (10)	1.00 (25)	1.6	33.8	8.4

ϖ is the activity coefficient defined as the ratio of enzyme, E, to the enzyme concentration at the beginning of being exposed to a defined temperature, E_o, $(\frac{E}{E_o})$. Other kinetic parameters such as half-life $(t_{1/2})$, decimal reduction time (D) values were obtained using the Eqs. (3) and (4)

$$t_{1/2} = In\ 2/k_d \tag{3}$$

$$D = In10/k_d \tag{4}$$

From Eq. (2) the activation energy of the irreversible enzyme inactivation (E_d) was derived from the slope of the plot of $Ink_d against\ 1/T$ for temperatures ranging from 40 to 80 °C. Other important thermodynamic parameters for free and immobilized cellulase and pectinase inactivation were determined using equations described below:

$$\Delta H_d^* = E_d - RT \tag{5}$$

$$\Delta G_d^* = -RTIn\left(\frac{k_d h}{k_b T}\right) \tag{6}$$

$$\Delta S_d^* = \frac{\Delta H^* - \Delta G^*}{T} \tag{7}$$

$\Delta H_d^*, \Delta G_d^*$ *and* ΔS_d^* are the activation enthalpy, Gibbs free energy and entropy respectively. Boltzmann constant (k_B) is 1.38 $\times 10^{-23}$ J^{-1} K^{-1}, Plank's constant (h) is 6.63 $\times 10^{-34}$ J^{-1} s^{-1} and the universal gas constant (R) is 8.314 $J^{-1}mol^{-1}K^{-1}$ [18].

The activation energy, E_a, was determined from the slopes of Arrhenius plot from the optimal temperature data (see Arrhenius equation below in Eq. (1)), In (k) vs 1/T, where k is the reaction rate and T is the temperature in Kelvin and A is the pre-exponential factor

$$In\ (k) = In\ A - \left(\frac{Ea}{R}\right)^1/_T \tag{8}$$

The temperature quotient, (Q_{10}), which is a factor that expresses rate increase when the temperature is increased by 10 °C [19] was estimated using the equation below

$$Q_{10} = Log^{-1}\left(\frac{E_a X 10}{RT^2}\right) \tag{9}$$

3. Results and discussion

3.1. Effect of different PEG molecular weight on a-amylase purification parameters

Different PEG with molecular weight ranging from 4000 to 8000 were investigated for its effect on the purification fold (PF), yield (Y) and partition coefficient (PC). The α-amylase was recovered at the top-phase and it was observed that increasing the PEG molecular weight above 6000 led to a decline in the PF, Y and PC (Fig. 1). PEG-6000 gave the highest PF, Y and PC while the use PEG-8000 resulted in decreased PF, Y and PC. A possible phenomenon for this observation is that the polymer has two distinguishing features namely its hydrophobic nature and stearic exclusion effect and this allowed for increased α-amylase partitioning in the lower phase. Increasing the molecular weight of the PEG above 6000 decreased the partition coefficient of the α-amylase. This is because of the volume exclusion effect via the reduced existing water content as the PEG molecular weight is increased. The overall effect is that the α-amylase migrates to the lower phase. The PF, Y and PC obtained when PEG-6000 was used were 2.4, 88% and 6.4 respectively. These values and observations were similar to that obtained for the ATPS purification of pineapple fruit bromelain [4] and white pitaya α-amylase [7]. Thus, PEG-6000 was selected after the screening process due to its higher purification fold, yield and partition coefficient values compared to PEG-4000 and PEG-8000.

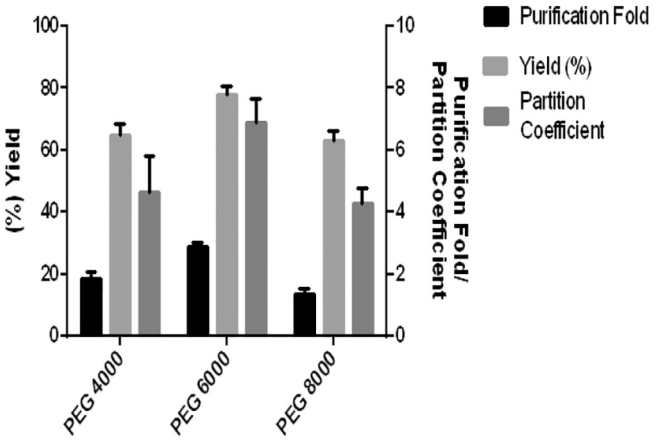

Fig. 1. The effect of different PEG molecular weight on partition coefficient, purification factor and yield of *Aureobasidium pullulans* α-amylase.

3.2. Response surface methodology

3.2.1. Regression analysis and fitting the response surface model

Multiple regression analysis was employed in this study to investigate the effects of PEG-6000, NaCl and sodium citrate concentration [Variables] on some α-amylase purification parameters such as yield, purification fold and partition coefficient [Responses]. Each individual response was further examined with respect to the linear, quadratic and interactions effects of these variables.

The regression equations are shown in below (Eqs. (10)–(12)). Analysis of variance (ANOVA) was used to determine the accuracy of the model.

$$\text{Purification Factor} = +4.09 - 0.5 * A + 0.43 * B + 0.47 * C - 1.42 * A2 - 1.17 * B2 - 0.96 * C2 - 0.44 * A * B - 0.024 * A * C - 0.11 * B * C \tag{10}$$

$$\%\text{Yield} = +87.75 - 12.45 * A + 8.57 * B + 9.77 * C - 30.50 * A2 - 26.31 * B2 - 19.51 * C2 - 10.99 * A * B - 1.43 * A * C - 2.56 * B * C \tag{11}$$

$$\text{Partition Coefficient} = +9.00 + 0.30 * A - 0.018 * B - 0.11 * C - 0.43 * A^2 - 0.71 * B^2 - 0.82 * C^2 + 0.00 * A * B + 0.46 * A * C - 0.036 * B * C \tag{12}$$

Table 3
Analysis of Variance (ANOVA) for the quadratic model for α-amylase partition coefficient.

Factor	Sum of squares	DF	Mean square	F-Value	Prob > F
Model	8.080	9	8.080	1231.98	<0.0001
A (NaCl)	0.740	1	0.740	1011.53	0.1035
B (citrate)	0.002	1	0.002	3.50	<0.0001
C (PEG-6000)	0.092	1	0.092	126.00	<0.0001
A * A	0.770	1	0.770	1061.08	<0.0001
B * B	2.150	1	2.150	2947.44	<0.0001
C * C	2.840	1	2.840	3897.99	<0.0001
AB	0.000	1	0.000	0.00	1.0000
AC	0.860	1	0.860	1183.03	<0.0001
BC	0.005	1	0.005	7.00	0.0331
Residual	0.005	7	0.007		
Lack of fit	0.005	3	0.001		0.189
Pure error	0.000	4	0.000		

R^2:0.9994; Adj R^2: 0.9986; Pred R^2: 0.9899; Adeq Precision: 102.

Table 4
Analysis of Variance (ANOVA) for the quadratic model for α-amylase % yield.

Factor	Sum of squares	DF	Mean square	F-Value	Prob > F
Model	12,491.67	9	1387.96	1291.90	<0.0001
A (NaCl)	1240.36	1	1240.36	1154.51	<0.0001
B (citrate)	586.92	1	586.92	546.30	<0.0001
C (PEG-6000)	763.16	1	763.16	710.34	<0.0001
A * A	3917.57	1	3917.57	3646.43	<0.0001
B * B	2914.52	1	2914.52	2712.80	<0.0001
C * C	1602.45	1	1602.45	1491.54	<0.0001
AB	483.50	1	483.50	450.04	<0.0001
AC	8.20	1	8.20	7.63	0.0280
BC	26.15	1	26.15	24.34	0.0017
Residual	7.52	7	1.07		
Lack of fit	4.59	3	1.53	2.09	0.2442
Pure error	2.93	4	0.73		

R^2:0.9974; Adj R^2: 0.9981; Pred R^2: 0.9938; Adeq Precision: 90.184.

The results are shown in Tables 3-5. The R^2 (Adj. and PrEd.) values obtained for the regression equations indicate a better and acceptable fitness of the models to the values obtained experimentally. The R^2 values obtained for all the responses (partition coefficient, purification fold and yield) were closer to 1 and it is interpreted that as the R^2 value gets closer to 1the model suggests a better response. For example, the R^2 value for the purification fold model is 0.991 (99%), this is interpreted as 99% of the variability in the response is explained by the model and the 1% that remains of the variability cannot be explained by the regression model. Similar observations can be made from the R^2 values obtained for the yield and partition coefficient models.

The lack of fit values obtained for all the response models in this study were not significant ($p < 0.05$), implying the higher level of adequacy of the model to predict possible variations in the responses. The Model F-values obtained for the partition coefficient, purification fold and yield were 1232, 884 and 1292 respectively and were significant (Tables 3-5). This means that there is only a 0.01% that Model-F values this large could occur due to noise. Value of "Prob > F″ < 0.05 indicate model terms were significant.

The liner, quadratic and interaction model term effects of PEG-6000, NaCl and sodium citrate concentration on the partition coefficient is explained in Tables 3-5. All the linear and quadratic model terms had significant effect on the partition coefficient, yield and purification fold. The least significant variable effects were the interaction models terms of both PEG-Citrate and Citrate-NaCl concentration for yield and purification fold. The least significant variable effects for the partition coefficient were PEG-Citrate and NaCl-Citrate concentrations. This observation and conclusion was also drawn by Shad et al. [7] where the quadratic effect of sodium chloride exhibited the most significant effect on partition coefficient.

Table 5
Analysis of Variance (ANOVA) for the Quadratic Model for α-amylase Purification Factor.

Factor	Sum of squares	DF	Mean square	F-Value	Prob > F
Model	26.750	9	2.97	883.54	<0.0001
A (NaCl)	2.570	1	2.570	764.68	<0.0001
B (citrate)	1.480	1	1.480	438.80	<0.0001
C (PEG-6000)	1.780	1	1.780	528.90	<0.0001
A * A	8.430	1	8.430	2506.53	<0.0001
B * B	5.720	1	5.720	1699.13	<0.0001
C * C	3.890	1	3.890	1157.64	<0.0001
AB	0.780	1	0.780	232.35	<0.0001
AC	0.002	1	0.002	0.68	0.4377
BC	0.047	1	0.047	13.68	0.0074
Residual	0.024	7	0.007		
Lack of fit	0.017	3	0.004	3.59	0.1244
Pure error	0.006	4	0.042		

R^2:0.9991; Adj R^2: 0.9980; Pred R^2: 0.9894; Adeq Precision: 76.244.

The 3-D response surface plots help provide the interactions between the independent variables while simultaneously making it easy to deduce the optimal levels for α-amylase extraction. The response surface plots are illustrated in Fig. 2(a-c) and the presence of elliptical contours in the plots is indicative of perfect interaction between the variables under consideration. Fig. 2a illustrates the effects of the independent variables (PEG and NaCl while Citrate is held constant) on the purification fold. From Fig. 2a, the presence of elliptical curves confirm that the purification fold is optimal at 15% PEG and 5% NaCl. Further increase over this optimal value led to a decline in the purification fold. Similar observations were made by both Navapara et al. [4] and Shad et al. [7]. Fig. 2b illustrates the effects of variables (PEG-Citrate while NaCl is held constant) on the partition coefficient. The volume effect plays a significant role in the α-amylase partitioning in the polyethylene glycol 6000 and citrate rich medium. The highest partition coefficient value was obtained at 15%PEG and 5% NaCl. It was observed that increasing the citrate concentration led to an increase in the partition coefficient. A possible explanation for this scenario is the salting out effect that allows for the increased movement of the biomolecules to the upper phase [20]. This observation whereby increased citrate led to increased partition coefficient was observed by Navapara et al. [4] and Shad et al. [7]. The effect of citrate and sodium chloride on yield is illustrated by the response surface plot in Fig. 2c. The central values of the variables gave the optimal yield. The optimum yield was obtained at 5% NaCl and 15% citrate. Overall, the optimal yield, purification fold and partition coefficient occurred at 20% PEG, 5% NaCl and 10% citrate.

3.2.2. Validation of the model for optimum purification fold, yield and partition coefficient

To validate the model, experiments were conducted under the conditions (optimum values of the independent variables) predicted by the regression equations. The ATPS was carried out using 20% (*w*/*v*) PEG, 7.5% (w/v) NaCl and 10% (w/v) sodium citrate. The experimental values obtained for the purification fold, yield and partition coefficient were 4.4, 88% and 9.0 respectively while the predicted values were 4.8, 87% and 8.7 for purification fold, yield and partition coefficient respectively. There were no significant difference between the experimental and actual values ($p < 0.05$) and it is concluded that the model was validated and appropriate for α-amylase purification. The crude and ATPS-partially purified α-amylase had activities of 120 0.5 ± 12.5 and 105.8 ± 9.5 Units respectively. The values obtained for the specific activities for crude and ATPS-partially purified α-amylase were 207.4 ± 9.5 and 995.6 ± 12.8 Units/mg respectively. Also, a comparative look at the bands present in the SDS-PAGE of the crude and partially purified α-amylase (Fig. 3) revealed that some level of purification by the ATPS system.

3.3. Effect of pH and temperature

The optimum temperature for both crude and ATPS-purified *A. pullulans* α-amylase obtained in this study was 50 °C (Fig. 4). The optimum temperature value obtained in this study was similar to that of *A pullulans Cau19* [11], *Laceyella sacchari TSI-2* [3] *and Trichoderma pseudokoningii* [21] α-amylase.

Fungal amylases are uniquely known to exhibit a pH optima ranging between acidity and alkalinity but in this study the optimum pH obtained for both crude and ATPS-purified *A. pullulans* α-amylase was 5.5 (Fig. 5). The value obtained in this study was different from that of *Laceyella sacchari TSI-2* [3] *and Trichoderma pseudokoningii* [21] α-amylase which both had a pH optima at 7.0. The difference noted in the optimum pH for fungal amylases might be associated with the type of fungus, environmental factors or its source of isolation.

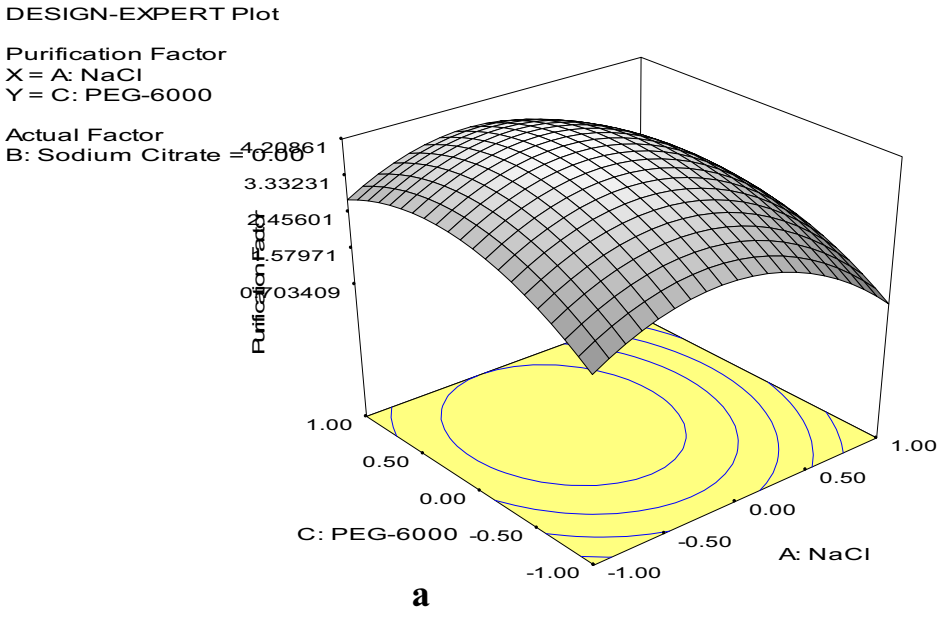

a

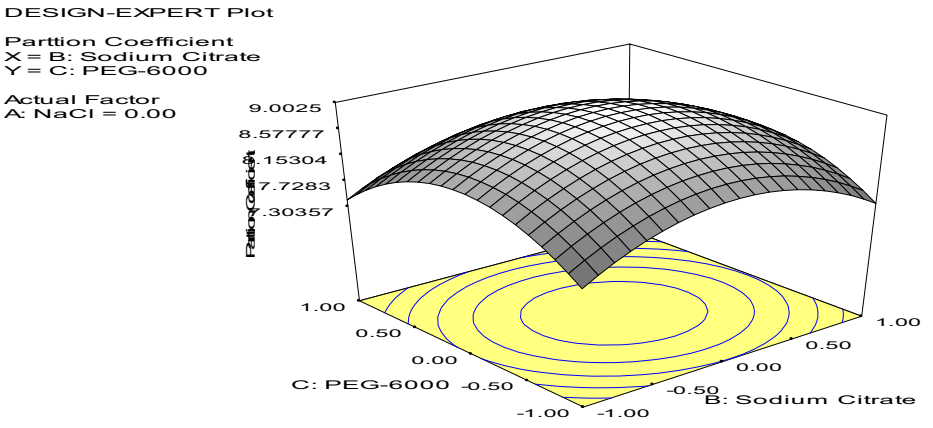

b

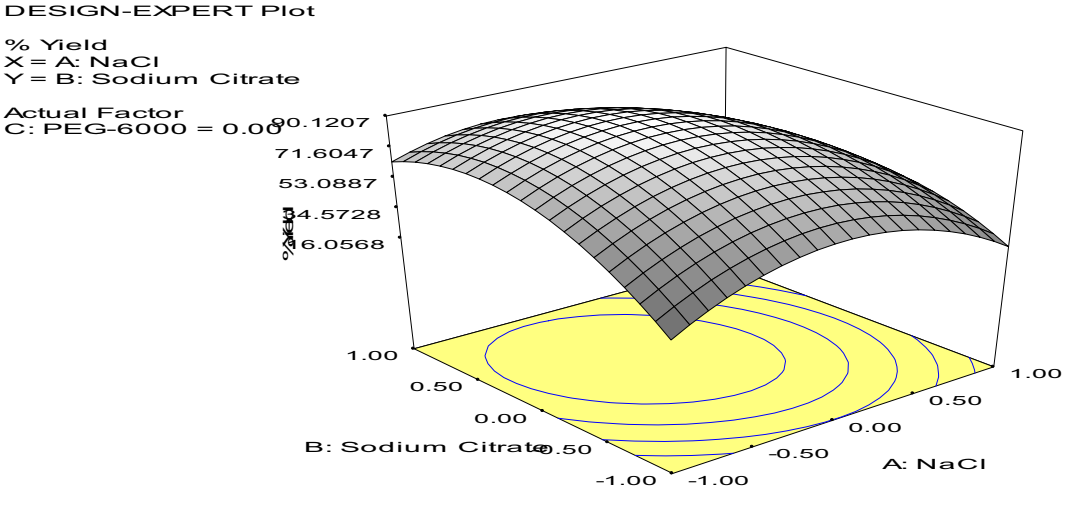

c

Fig. 2. (a) Three-dimensional response surface plots for the combinatorial effects of sodium chloride and PEG-6000 on the purification effect (b). Three-dimensional response surface plots for the combinatorial effects of sodium citrate and PEG-6000 on the partition coefficient. (c). Three-dimensional response surface plots for the combinatorial effects of sodium chloride and sodium citrate on the %yield.

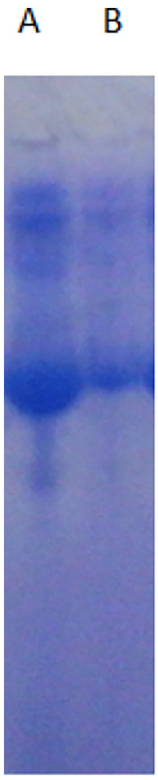

Fig. 3. SDS-PAGE of crude amylase (lane A) and ATPS-partially purified α-amylase (lane B).

3.4. Kinetic and thermodynamic properties of ATPS purified A. pullulans α-amylase

It is important that enzymes for industrial application must possess some unique properties such as resistance to thermal inactivation which is often reflected in terms of their thermodynamic and kinetic parameters. From the semi-log plots of the $In\frac{E}{E_o}$ against *time*, it was noted that the α-amylase activity for both crude and ATPS-purified typified first-order denaturation kinetics (Fig. 6a & b) and this observation was also noted by Oliviera et al. [22] and Pal and Khrum [23]. A summary of the kinetic and thermodynamic properties is shown in Table 6.

3.4.1. Kinetic properties for A. pullulans α-amylase thermal inactivation

As obtained in this study, the first-order thermal inactivation constant (k_d) increased gradually from 50 °C while the half-life ($t_{1/2}$)

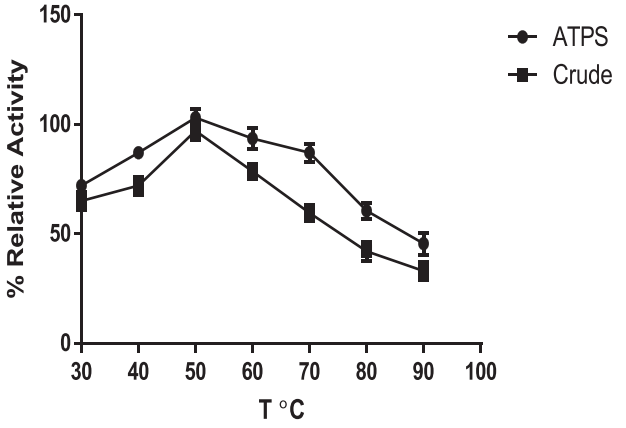

Fig. 4. Effect of temperature on crude and ATPS partitioned *A. pullulans* α-amylase.

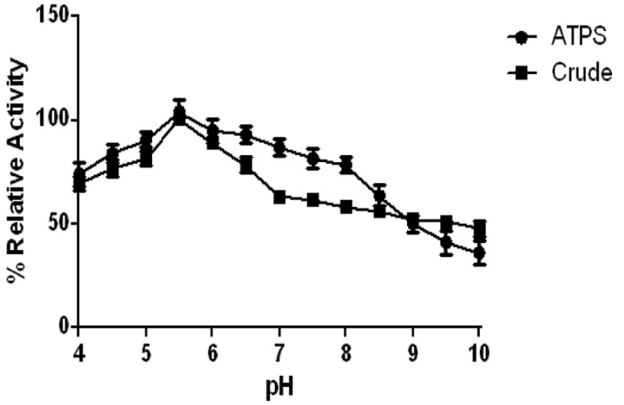

Fig. 5. Effect of pH on crude and ATPS partitioned *A. pullulans* α-amylase.

decreased [24]. This implied that thermal inactivation caused a gradual decline in the thermal stability. The $t_{1/2}$is defined as the time after which the enzyme activity was reduced to one-half of the initial activity. In this study, as temperatures rose above 50 °C the half-life decreased from 15 h to 9.2 h for the ATPS-purified and 5.1 to 2.6 for the crude α-amylase. The results obtained for the $t_{1/2}$for *A. pullulans* α-amylase was similar to that obtained for *Thermoactinomycetes vulgaris* [25] which was thermostable at 50 °C but lower than *L. sacchari* TSI-2 amylase was thermostable at 70 °C. Several factors influence enzyme thermostability and it could be a mix of biomolecules present, surrounding environmental factors, increased concentration of proteins etc. [3]. The decimal reduction time (D-value) is another important kinetic parameter estimated in this study and it is defined as the time of exposition of enzyme at a specific temperature necessary to maintain 10% residual activity [23]. As seen in Table 2, there was a good thermal stability at 50 and 60 °C because more time was needed (19.4 h) for the ATPS purified α-amylase to reach a 10% reduction of the initial activity while a relatively shorter time (2.9 h). This implies that, the ATPS-purified enzyme

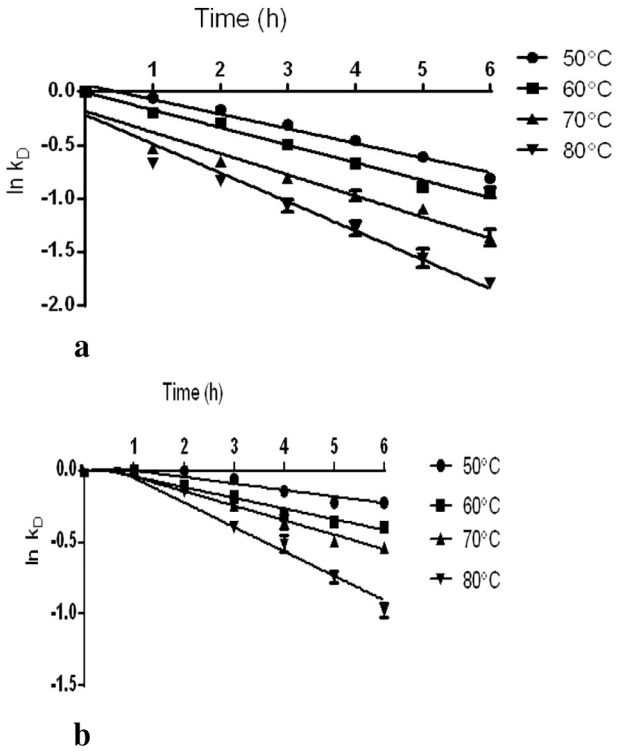

Fig. 6. a. Semi-log plots of thermal denaturation of crude *A. pullulans* α-amylase. b. Semi-log Plots of thermal denaturation of ATPS purified *A. pullulans* α-amylase.

Table 6
Kinetic and thermodynamic parameters for ATPS purified *A. pullulans* α-amylase.

T (K)	k_D (h^{-1})	R^2	$t_{1/2}$ (h)	$D-value$ (h)	E_d $(\frac{kJ}{mol})$	ΔH_d $(\frac{kJ}{mol})$	ΔG_d $(\frac{kJ}{mol})$	ΔS_d $(\frac{J}{mol/K})$
ATPS								
323	0.045	0.866	15.0	51.6	51.9	49.2	87.6	−118.9
333	0.075	0.9601	9.2	30.7	($R^2 = 0.888$)	49.1	89.0	−119.8
343	0.102	0.9583	6.8	22.6		49.0	90.9	−122.2
353	0.170	0.9576	4.1	13.5		48.9	92.1	−122.3
Crude								
323	0.1366	0.9744	5.1	16.9	28.6	25.9	53.6	−85.8
333	0.1643	0.9820	4.2	14.0	($R^2 = 0.957$)	25.8	54.7	−86.9
343	0.1986	0.9356	3.5	11.6		25.7	55.7	−87.5
353	0.2712	0.9526	2.6	8.5		25.7	56.3	−86.7

was thermally resistant than the crude. Further increase in the temperature above 60 °C led to a sharp decline in the D-values. The activation energy,E_a value obtained from the Arrhenius plot of In (Activity) against 1/T was 14.56 kJ/mol/K for ATPS-purified and 16.22 kJ/mol/K for the crude α-amylase (Fig. 7a & b). The value of E_a obtained for *Bacillus licheniformis* SKB4 α-amylase was 31.53 kJ/mol/K [26]. The value obtained in our study was relatively low and it implied that very few energies were effectively utilized to form the activated complex Pal and Khrum [23]. The temperature quotient, Q_{10} is often used as a yardstick to determine if there were extraneous factors aside temperature influencing catalytic reaction by enzymes as well as the temperature dependency of such reactions [19]. The Q_{10} values range between 1and 2 for reactions totally dependent on temperature. In this study the Q_{10} values were between 1 and 1.2 both crude and ATPS-purified and this signifies that the enzymatic reactions were totally dependent only on temperature and not on other extraneous factors.

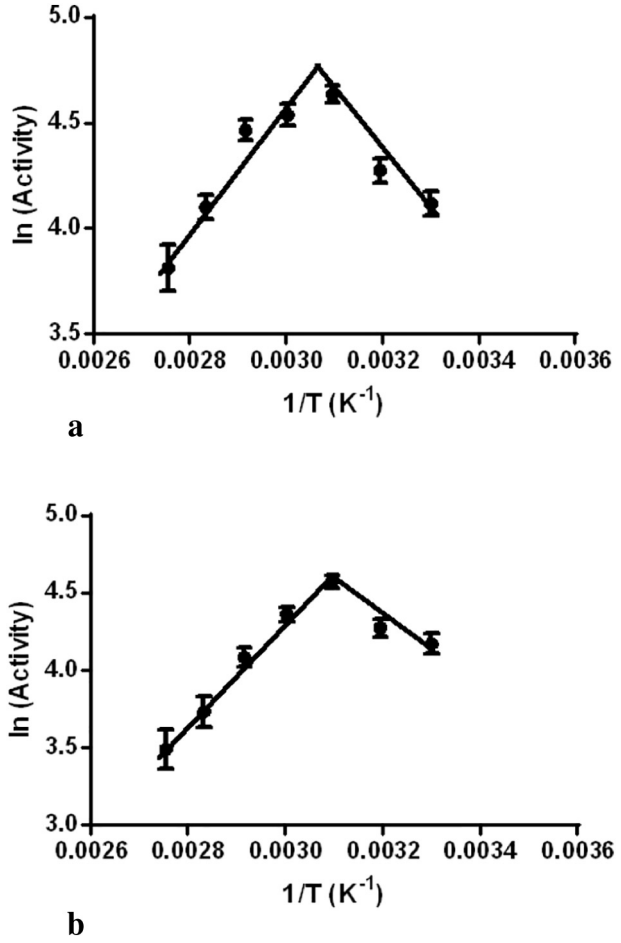

Fig. 7. a. Arrhenius-type plot for the estimation of the activation energy for ATPS-purified α-amylase. b. Arrhenius-type plot for the estimation of the activation energy for crude α-amylase.

3.4.2. Thermodynamic properties for A. pullulans α-amylase thermal inactivation

The activation energy of thermal inactivation, E_d^*, is the minimum amount of energy needed for a typical heat inactivation process and it is a barrier important for the stability of enzymes. An important implication of overcoming this barrier is that once this barrier had been overcome, the thermally denatured enzyme cannot refold back into its native state. The E_d^* obtained for the ATPS-purified and crude α-amylase were 51.9 kJ/mol (R^2= 0.888) and 29.8 kJ/mol (R^2= 0.957) as seen in Table 6 and Fig. 8. It can be concluded that the positive values of E_d^* indicate thermostability [22]. The relatively high E_d^* value for the ATPS-purified α-amylase compared to the crude enzyme suggests that the ATPS-purified enzyme was more resistant to thermal inactivation and that probably its 3-D structure was relatively unperturbed by heat. ATPS purification is known to confer thermostability on biomolecules [4] and this increased resistance to thermal denaturation was observed for the ATPS-purified α-amylase. The same argument is also tenable for the activation enthalpy of deactivationΔH_d^* since they both closely related ($\Delta H_d^* = E_d^* - RT$) i.e. a positive value of ΔH_d^* (48.9–49.2 for ATPS-purified and 25.7–25.9 for crude α-amylase) obtained in this study is often associated with high thermal stability. It was observed that there was a progressive decrease in the ΔH_d^* values and this meant that the α-amylase (both ATPS-purified and crude) was highly thermal stable because little energy was needed to thermally inactivate the enzyme. A similar observation was noted for pectinase from *Aspergillus oryzae* [22]. Thermal inactivation of biomolecules is often a cascade of events that lead to the disruption of covalent and non-covalent linkages (hydrophobic interactions) hence resulting in increased ΔH_d^*. Also, since the minimum energy needed to remove a CH_2-

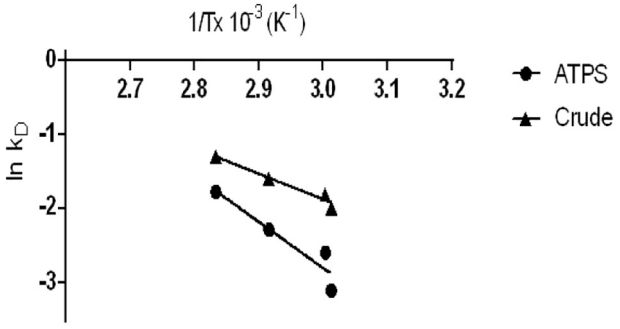

Fig. 8. Arrhenius plot to estimate the thermodynamic parameters of thermal denaturation of crude and ATPS partitioned *A. pullulans* α-amylase.

molecule from a hydrophobic bond is approximately 5.4 kJ/mol [27,28], the average non-covalent bonds disrupted was calculated as 9.1 and 5.1 for the ATPS-purified and crude α-amylase respectively. The values obtained in this study compares well with the values obtained for free and immobilized pectinase from *Aspergillus oryzae* which were 15.3 and 18.3 respectively [22].

A feature associated with thermal deactivation of enzymes is the unfolding of the three-dimensional structure of the protein and this process is often accompanied by an increase in the degree of disorderliness (often time indicated by the large and positive entropy values, ΔS_d^*). In this study, the values obtained for the ΔS_d^* for partially purified α-amylase were negative (from −118.9 to −122.3) for ATPS-purified and (from −85.8 to −86.7) indicating higher orderliness of the activated complex as well as its thermal stability at the temperatures considered.

The Gibbs free energy of thermal inactivation, ΔG_d^*, is a better parameter to determine the thermal stability of enzymes because it is often derived from two important parameters namely ΔH_d^* *and* ΔS_d^* obtained from the equation: $\Delta G_d^* = \Delta H_d^* - T\Delta S_d^*$ [16]. Increase in the ΔG_d^* values are associated with increases potentials of the enzyme to withstand thermal inactivation while negative values indicate that the enzyme was susceptible to thermal inactivation albeit simultaneously [22,28]. The values obtained in this study for the ATPS purified and crude α-amylase range from 87.6 to 92.1 and 53.6–56.3 respectively (Table 6) and it compares well with the thermal stable α-amylase from *L. sacchari* TSI-2 which had ΔG_d^* values ranging from 76.02 to 82.32 [3]. Hence it is concluded that the ATPS-purified α-amylase withstood thermal inactivation and it is thermally stable at the temperatures considered.

4. Conclusion

Enzymes for industrial applications must be easily purified and concentrated and in this study ATPS was employed. PEG-6000 was the best polymer for partitioning of the crude α-amylase as it gave higher yield, purification factor and partition coefficient. After optimization of the process for ATPS, the best combination of factors that gave highest yield, partition coefficient and purification factor were PEG-6000 [20%]; NaCl [7.5%] and sodium citrate [10%]. The model was validated and suitable for ATPS partitioning of *A. pullulans* alpha-amylase. Overall, when both kinetic and thermodynamic parameters are taken into consideration, the ATPS partitioned α-amylase was more thermally stable than the crude and this makes its application for numerous industrial applications exploitable.

References

[1] S. Kumar, S, Khare, Chloride activated halophilic alpha-amylase from *Marinobacter* sp. EMB8: production, nanoimmobilization for efficient starch hydrolysis. Enzyme Research..doi:https://doi.org/10.1155/2015/859485.

[2] M. Hashemi, S.M. Mousavi, S.H. Razavi, S.A. Shojaosadati, Comparison of submerged and solid state fermentation systems effects on the catalytic activity of *Bacillus* sp. KR-8104 a-amylase at different pH and temperatures. Ind. Crop. Prod. 43 (2013), 661–667. doi:https://doi.org/10.1016/j.indcrop.2012.08.002.

[3] R.J. Shukla, S.P. Singh, Characteristics and thermodynamics of alpha-amylase from thermophilic actinobacterium, *Lacyella sacchari* TSI-2. Process Biochem.. doi: https://doi.org/10.1016/j.procbio.2015.10.013.

[4] D.R. Navapara, D.N. Avhad, V.K. Rathod, Application of response surface methodology for optimization of bromelain extraction in aqueous two-phase system, Sep. Sci. Technol. 46 (11) (2011) 1838–1847, https://doi.org/10.1080/01496395.2011.578101.

[5] A. Rito, M. Palmares, Practical application of aqueous two phases partition to process development for the recovery of biological products–a review, J. Chromatogr. B 807 (2004) 3–11.

[6] A. Salabat, M.H. Abnosi, A.R. Bahar, Amino acids partititoning in aqueous two-phase system poly propylene glycol and magnesium sulfate, J. Chromatogr. B 858 (2007) 234–238.

[7] Z. Shad, H. Mirhosseini, A.S.M. Hussin, B. Forghani, M. Motshakeri, M.Y. Abdul Manap, Aqueous two-phase purification of a-amylase from white pitaya (*Hylocereus undatus*) Peel in polyethylene glycol/citrate system: optimization by response surface M e t h o d o l o g y, Biocatalysis and Agricultural Biotechnology. doi: https://doi.org/10.1016/j.bcab.2018.01.014.

[8] W. Zhang, X. Liu, H. Fan, D. Zhu, X. Wu, X. Huang, J. Tang, Separation and purification of alkaloids from Sophora flavescens by focused microwave-assisted aqueous two-phase extraction coupled with reversed micellar extraction, Ind. Crop. Prod. 86 (2016) 231–238, https://doi.org/10.1016/j.indcrop.2016.03.052.

[9] G. Tubío, B. Nerli, G. Picó, Partitioning features of bovine trypsin and a-chymotrypsin in polyethyleneglycol-sodium citrate aqueous two-phase systems, J. Chromatogr. B 852 (2007) 244–249, https://doi.org/10.1016/j.jchromb.2007.01.025.

[10] N.L. Loc, N.T.T. Mien, D.T.B. Thuy, Purification of extracellular a-amylase from Bacillus subtilis by partitioning in a polyethylene glycol/potassium phosphate aqueous two-phase system, Anal Microbiol 60 (2010) 623–628, https://doi.org/10.1007/s13213-010-0100-x.

[11] Y.R. Mulay, R.I. Deopurkar, Purification, characterization of amylase from indigenously isolated *Aureobasidium pullulans* Cau 19 and its bioconjugates with gold nanoparticles. Appl. Biochem. Biotechnol. DOI https://doi.org/10.1007/s12010-017-2575-4.

[12] A.N. Ademakinwa, Z.A. Ayinla, F.K. Agboola, Strain improvement and statistical optimization as a combined strategy for improving fructosyltransferase production by *Aureobasidium pullulans* NAC8, J. Genet. Eng. Biotechnol. 15 (2017) 341–353, https://doi.org/10.1016/j.jgeb.2017.06.012.

[13] G. Miller, Use of dinitrosalicylic acid reagent for determination reducing sugar, Anal. Chem. 31 (1959) 426–428, https://doi.org/10.1021/ac60147a030.

[14] M.M. Bradford, A rapid and sensitive method for the quantitation of microgram quantities of protein utilizing the principle of protein-dye binding, Anal. Biochem. 72 (1976) 248–254, https://doi.org/10.1016/0003-2697(76)90527-3.

[15] U.K. Laemmli, Cleavage of structural proteins during the assembly of the head of bacteriophage T4, Nature 227 (1970) 680–685.

[16] P.M. Souza, B. Aliakbarian, E. Ximenes, F. Filho, P. Oliveira, A. Pessoa, A. Converti, Kinetic and thermodynamic studies of a novel acid protease from Aspergillus foetidus, Int. J. Biol. Macromol. 81 (2015) 17–21, https://doi.org/10.1016/j.ijbiomac.2015.07.043.

[17] T.S. Porto, C.S. Porto, M.T.H. Cavalcanti, J.L.L. Filho, P. Perego, A.L.F. Porto, A. Converti, A. Pessoa, Kinetic and thermodynamic investigation on ascorbate oxidase activity and stability of a *Cucurbita maxima* extract, Biotechnol. Prog. 22 (2006) 1637–1642, https://doi.org/10.1021/bp0602350.

[18] M. Melikoglu, C.S.K. Lin, C. Webb, Kinetic studies on the multi-enzyme solution produced via solid state fermentation of waste bread by Aspergillus awamori, Biochem. Eng. J. 80 (2013) 76–82, https://doi.org/10.1016/j.bej.2013.09.016.

[19] H.R. Wehaidy, M.A. Abdel-Naby, W.G. Shousha, M.I.Y. Elmallah, M.M. Shawky, Improving the catalytic, kinetic and thermodynamic properties of Bacillus subtilis KU710517 milk clotting enzyme via conjugation with polyethylene glycol, Int. J. Biol. Macromol. 111 (2018) 296–301, https://doi.org/10.1016/j.ijbiomac.2017.12.125.

[20] I.P. Trindade, M.M. Diogo, D.M.F. Prazeres, J.C. Marcos, Purification of plasmid DNA vectors by aqueous two-phase extraction and hydrophobic interaction chromatography, J. Chromatogr. A 1082 (2005) 176–184, https://doi.org/10.1016/j.chroma.2005.05.079.

[21] A.H. Wessam, Purification and characterization of alpha-amylase from *Trichoderma pseudokoningii*, BMC Biochem. 19 (4) (2018) 1–6, https://doi.org/10.1186/s12858-018-0094-8.

[22] R.L. Oliveira, O.S. da Silva, A. Converti, T.S. Porto, Thermodynamic and kinetic studies on pectinase extracted from Aspergillus aculeatus: free and immobilized enzyme entrapped in alginate beads, Int. J. Biol. Macromol. 115 (2018) 1088–1093, https://doi.org/10.1016/j.ijbiomac.2018.04.154.

[23] A. Pal, F. Khanum, Covalent immobilization of xylanase on glutaraldehyde activated alginate beads using response surface methodology: characterization of immobilized enzyme, Process Biochem. 46 (2011) 1315–1322, https://doi.org/10.1016/j.procbio.2011.02.024.

[24] S.D. Gohel, S.P. Singh, Characteristics and thermodynamics of a thermostable protease from a salt-tolerant alkaliphilic actinomycete, Int. J. Biol. Macromol. 56 (2013) 20–27, https://doi.org/10.1016/j.ijbiomac.2013.01.028.

[25] B.A. Kikani, B.P. Singh, The stability and thermodynamic parameters of a very thermostable and calcium independent a-amylase from a newly isolated bacterium, *Anoxybacillus beppuensis* TSSC-1, Process Biochem. 47 (2012) 1791–1798.

[26] S. Samamtha, A. Das, S.K. Halder, A. Jana, S. Kar, P.K.D. Monapatra, B.R. Pat, K.C. Mondal, Thermodynamic and kinetic characteristics of an alpha-amylase from bacillus licheniformis SKB4, Acta Biol Szeged. 58 (2014) 147–156.

[27] C.N. Pace, Contribution of the hydrophobic effect to globular protein stability, J. Mol. Biol. 226 (1992) 29–35, https://doi.org/10.1016/0022-2836(92)90121-Y.

[28] A.N. Ademakinwa, F.K. Agboola, Kinetic and thermodynamic investigations of Cell-Wall degrading enzymes produced by *Aureobasidium pullulans* via induction with Orange peels: application in lycopene extraction, Prep. Biochem. Biotechnol. (2019)https://doi.org/10.1080/10826068.2019.1650375.